

Contents lists available at [ScienceDirect](http://ScienceDirect.com)**Physica C**journal homepage: www.elsevier.com/locate/physc

Depairing current density of $\text{Ba}_{0.5}\text{K}_{0.5}\text{Fe}_{1.95}\text{Co}_{0.05}\text{As}_2$ microbridges with nanoscale thickness



Jun Li ^{a,b,*}, Jie Yuan ^b, Jun-Yi Ge ^a, Min Ji ^{b,c}, Hai-Luke Feng ^{b,d}, Ya-Hua Yuan ^{b,d}, Takeshi Hatano ^b, Johan Vanacken ^a, Kazunari Yamaura ^{b,d}, Hua-Bing Wang ^{b,c}, Eiji Takayama-Muromachi ^{d,e}, Victor V. Moshchalkov ^a

^a INPAC – Institute for Nanoscale Physics and Chemistry, KU Leuven, Celestijnenlaan 200D, B-3001 Leuven, Belgium

^b Superconducting Materials Center, National Institute for Materials Science, 1-1 Namiki, Tsukuba, Ibaraki 305-0044, Japan

^c Research Institute of Superconductor Electronics, Nanjing University, Nanjing 210093, China

^d Department of Chemistry, Graduate School of Science, Hokkaido University, Sapporo, Hokkaido 060-0810, Japan

^e International Center for Materials Nanoarchitectonics (WPI-MANA), National Institute for Materials Science, 1-1 Namiki, Tsukuba, Ibaraki 305-0044, Japan

ARTICLE INFO

Article history:

Received 12 December 2013

Received in revised form 26 March 2014

Accepted 27 March 2014

Available online 15 April 2014

Keywords:

Fe-pnictide

Superconductor

Doping

Critical current density

ABSTRACT

We investigated the depairing current density of $\text{Ba}_{0.5}\text{K}_{0.5}\text{Fe}_{1.95}\text{Co}_{0.05}\text{As}_2$ microbridges with width of 2 μm and thickness of 150 nm. The current vs. voltage characteristics of the microbridges show a Josephson-like behavior with the obvious hysteresis. The critical current density was observed as $J_c = 7.9 \text{ MA/cm}^2$ at temperature 21 K, which is consistent with the Ginzburg–Landau depairing limit. However, the depairing current density is less than that of impurity-free crystal, although the Co ions provide additional pinning centers within the superconducting Fe_2As_2 layers. The Co impurity also enhances the anisotropic factor of the critical current density by 1.3 (1 T) or 1.7 (3 T).

© 2014 Elsevier B.V. All rights reserved.

1. Introduction

Recently, the high- T_c Fe-based superconductors attracted increasingly more attentions for the possible applications, owing to high superconducting transition temperature (T_c), high upper critical fields (H_{c2}), low anisotropic factor, and high critical current density (J_c) [1–3]. Compared with the layered cuprates family, although Fe-based superconductors have relatively lower T_c , they demonstrate nearly isotropic behavior [2,3]. Previously, the highest J_c of Fe-based superconductors was reported as less than 10 MA/cm² at 4.2 K [4–8], based on the data obtained from transport properties of thin film micro-device and magnetization hysteresis loop (MHL) measured on bulk single crystals. For the former, although the thin films were fabricated successfully for several systems, such as Fe(Se, Te) [4], Ba(Fe, Co)₂As₂ [5–7], and LaFeAsO_{1-x}F_x [8], one can hardly obtain an ideal single-crystalline film due to the appearance of additional grain boundaries resulting from the island-like growth process [9,10]. The J_c may be enhanced by the

existence of grain boundaries, while the critical current exhibits exponential decay in the weak-link regime which is a critical issue for practical applications. Consequently, it is rather difficult to elucidate the intrinsic physical properties of the superconductors. The latter method is to measure the J_c indirectly from magnetization hysteresis loop (MHL) on single crystals, namely, evaluation from the magnetic vortex penetration features into the crystal by using the Bean model [11], where the vortex penetration is mainly determined by pinning which depends on various parameters, such as the presence of defects, grain boundaries, and geometry of the materials.

We stress that both methods for the J_c evaluation are limited by the vortex moving features under finite pinning force, which is generally far away from the intrinsic transporting capability, namely, the Ginzburg–Landau (GL) depairing current density (J_c^{GL}). Previous estimation from $J_{ab}^{\text{GL}} = \Phi_0/3\sqrt{3}\pi\mu_0\lambda_{ab}^2\xi_c$ [12] (where λ_{ab} and ξ_c are the in-plane penetration depth and out-of-plane coherence length, respectively) shows that J_c^{GL} could be as high as 200 MA/cm² at absolute zero temperature for (Ba, K)Fe₂As₂ [12], thus indicating about two orders of magnitude larger values than those derived from previous experimental J_c . Generally, it is rather difficult to reach the J_c^{GL} , even for the conventional superconductors and the cuprates [13]. J_c^{GL} is extremely sensitive to crystal quality, while

* Corresponding author at: INPAC – Institute for Nanoscale Physics and Chemistry, KU Leuven, Celestijnenlaan 200D, Box 2414, BE – 3001 Leuven, Belgium. Tel.: +32 16 327 260; fax: +32 16 327 983.

E-mail address: Jun.Li@fys.kuleuven.be (J. Li).

the Fe-based single crystals were often found to contain microscopic and even intrinsic defects. In addition, to obtain the J_c^{GL} the size of the crystal should be adjusted below the Pearl length $\Lambda = 2\lambda^2/h$ (λ and h are the London penetration depth and thickness of the bridge, respectively [14–16]). Recently, we developed a micro-patterned method using the $\text{Ba}_{0.5}\text{K}_{0.5}\text{Fe}_2\text{As}_2$ single crystals [17]. The J_c^{GL} is increased up to 10.8 MA/cm^2 at 35 K and reaches 944.4 MA/cm^2 by extrapolating $J_c(T)$ to $T = 0$ once the thickness of the microbridge (91 nm) is below to the Pearl length.

In the present work, we report on the observation of J_c^{GL} in Co-doped $\text{Ba}_{0.5}\text{K}_{0.5}\text{Fe}_2\text{As}_2$ superconductors. We found that the 150 nm thin microbridges demonstrate an individual jump from superconducting (SC) to normal state directly with the absence of flux-flow behavior in the current (I) and voltage (V) characteristics (IVCs) curves, and the J_c is enhanced up to 7.9 MA/cm^2 at 21 K, which is quite close to the GL depairing limit. We have investigated the temperature dependences and anisotropy of J_c .

2. Experimental

The synthesis process of $\text{Ba}_{0.5}\text{K}_{0.5}\text{Fe}_{1.95}\text{Co}_{0.05}\text{As}_2$ single crystals was described elsewhere [18]. However, we improved the high-pressure synthesis technique for high quality single crystals recently, i.e., the samples were kept at 1300°C for 4 h, and then slowly cooled down to 1100°C for 2 h before quenched to room temperature. In the first process, the Co ions can be homogeneously distributed within the superconducting Fe_2As_2 layers to reduce the effect of disorder. For the fabrication of microbridges we utilized the same method as introduced in a recent work [17]. The crystal was firstly cleaved into pieces of $0.5\text{--}1 \mu\text{m}$ in thickness along the c -axis and pasted on a Si substrate using a thin layer of epoxy glue. The as-prepared crystal was removed a layer of 10 nm using the low energy argon ion beam and then a 100 nm layer of Au was deposited on the sample surface immediately. The sample was annealed at 300°C for 24 h under nitrogen atmosphere to reduce the interface contact resistance between gold and crystal, and as a result, the contact resistance was decreased to 0.5Ω at room temperature. The micro-bridge patterns were fabricated on the as-prepared single crystals using the photolithography technique, where the geometry of microbridges is with width (W) of $2 \mu\text{m}$ and length (L) of $10 \mu\text{m}$. Then, the photoresist was removed using acetone and the electrodes were connected using silver epoxy. Finally, the whole device was milled into a certain thickness. We determined the thickness based on the ion-milling rate and room temperature resistance in the same way as described in our previous work [17]. The transport properties, including the temperature

and magnetic field dependence of in-plane resistivity (ρ_{ab}) and IVCs, were measured in the Physical Properties Measurement System – 9 T, Quantum Design.

3. Results and discussions

Fig. 1 shows $\rho_{ab}(T)$ curves for the microbridge with thicknesses (h) of 150 nm. The values of ρ_{ab} are about one order magnitude less than the bulk crystals. This reduction can be attributed to improvement of the crystal synthesis technique and measurement setup. In the traditional four-probe measurement, a high current bias was often necessary to enhance the measurement resolution, owing to the big sample size and strongly metallic behavior of the crystals. In this case, the heating effects can be quite substantial, particularly at the interface between silver paste and crystal [17]. For the present measurement setup, however, the resistance of microbridge is relatively large, for instance, 29.5Ω at room temperature, thus one can apply current as low as $10 \mu\text{A}$. Moreover, the interface contact resistance is less than 0.5Ω at room temperature, which will be even less at low temperatures and therefore can be omitted. Particularly, the electrodes are SC as well [17]. Consequently, we can reduce the heating effects.

The T_c -onset for the microbridge with thickness of 150 nm is $\sim 28 \text{ K}$, slightly less than our previously reported value, suggesting more homogenous distribution of the impurity ions and decrease of disorder. Indeed, we measured the bulk-like microbridges with thickness up to $1 \mu\text{m}$, and the T_c -onset is in accordance with the present result. However, the SC transition width ΔT_c of the sample with thickness of 150 nm is surprisingly large, about 5 K, while in the bulk crystal ΔT_c is normally $\sim 0.2 \text{ K}$ (not shown here). In addition, the $\rho_{ab}(T)$ curves demonstrate several platform-like steps within the transition region, after the initial drop at the T_c -onset. Such platform-like steps in the $\rho_{ab}(T)$ curves were widely found in low- T_c nanowires [19–21] and high- T_c $\text{YBaCu}_3\text{O}_{7-\delta}$ microbridges [22], which were explained as thermally activated phase-slip (PS) centers or lines which can induce resistance. On the other hand, the steps are weakened by applying magnetic field, and such phenomenon is more obvious for the case of the $H//ab$ -plane field orientation than for the $H//c$ -axis. As field increases, the T_c is gradually suppressed regardless the direction of the field, while transition regions are observed as almost constant for $H//ab$ -plane but slightly broadened for $H//c$ -axis, due to layered crystal structure.

Fig. 2 shows the IVCs at various temperatures from 21 to 26 K. At relatively low temperature of 21 K, the voltage state is switched from SC to normal state directly with the absence of flux-flow process, and the J_c reveals high value of 7.9 MA/cm^2 . According to our

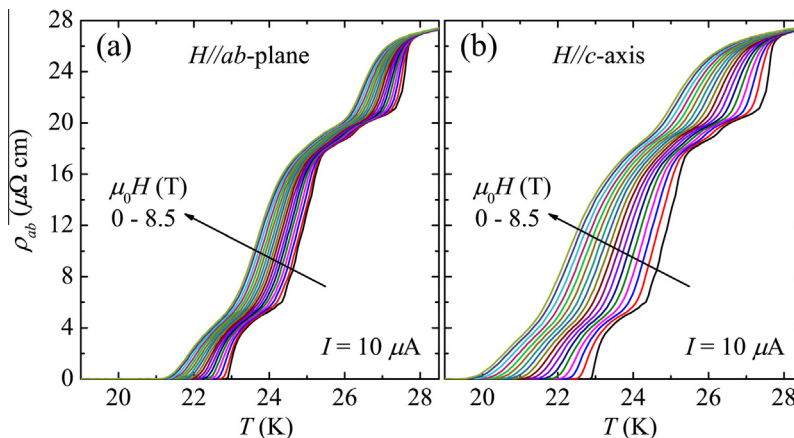


Fig. 1. Temperature dependence of the in-plane magnetoresistivity $\rho_{ab}(T)$ for microbridge with thickness of 150 nm. The applied current is $10 \mu\text{A}$ for all measurements, and the fields are applied within the ab -plane for (a) and along c -axis for (b).

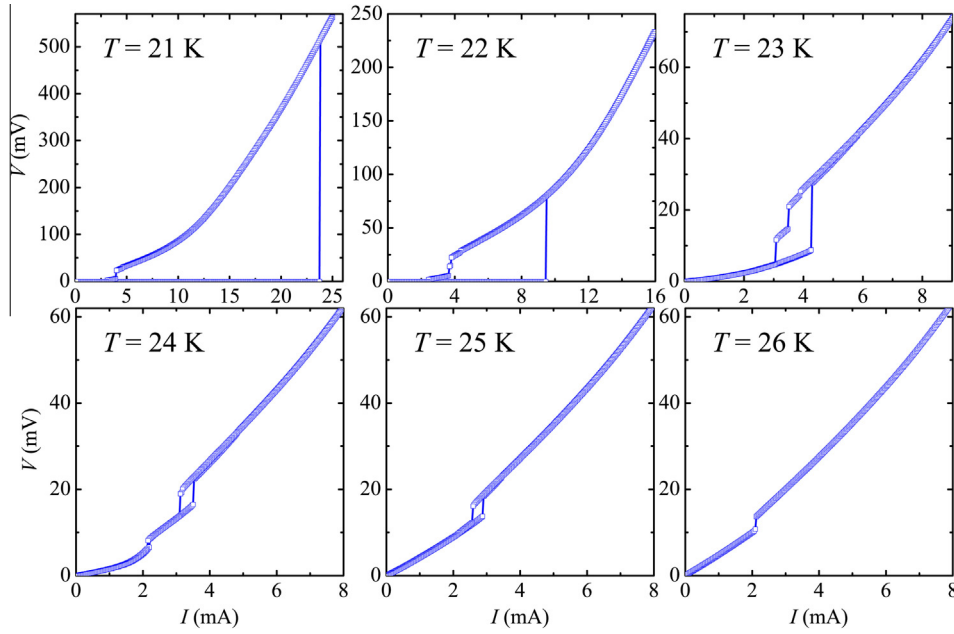


Fig. 2. Current–voltage characteristics for the microbridges at temperatures from 21 to 26 K.

previous study on the $\text{Ba}_{0.5}\text{K}_{0.5}\text{Fe}_2\text{As}_2$ single-crystalline microbridges [17], such voltage state behavior is in accordance with the transition of the GL depairing current density. On the other hand, when the current is swept down, the voltage returns from the normal to the SC state, followed by a pronounced hysteretic resistance state. As temperature increasing only 1 K, the J_c however declines to more than half (3.2 MA/cm^2), indicating that the J_c is quite sensitive to temperatures. Indeed, such behavior was also found for the J_c^{GL} of $\text{Ba}_{0.5}\text{K}_{0.5}\text{Fe}_2\text{As}_2$. Note that there are two steps on the return branch. The pronounced hysteresis of IVCs exhibits the kinetics of the joule heating processes, which dominate the instantaneous dissipations in the mesoscopic system and then influence the PS kinetics. The thermally activated PS often happens at temperatures slightly below the T_c , for which the spatiotemporal fluctuations of order parameter are intensive. Once at finite low temperatures, the thermal energy $k_B T$ becomes too low to provide the enough energy for the occurrence of PS, current switch may then depend on the limit of the J_c^{GL} . Alternatively the quantum tunneling through the energy barrier can also result in a directly SC-normal state switching [19–21]. However, in that case the sample should be in a one-dimensional or quasi-one-dimensional geometry with characteristic size comparable to ξ . From this point of view we can hardly observe a quantum phenomenon in the present microbridge due to the extremely small ξ ($\sim 1.5 \text{ nm}$ at 0 K), which is close to the size of a unit cell of the crystal. As the temperature increase to 23 K, an obvious flux-flow phenomenon is observed before the first jump to the normal state and the PS steps on the return branches are pronounced as well. For the temperatures above 23 K, the flux-flow contribution becomes quite large, owing to the thermal activation near the T_c .

In Fig. 3 we give the differential resistances of microbridges at various temperatures and applied current densities, where the data points reveal each resistance shunt and correspond to the J_c s. The J_c at temperature of $T/T_c = 0.75$ is 7.9 MA/cm^2 , which is visibly less than that of impurity-free crystal around the T_c , for instance, $J_c = 10.8 \text{ MA/cm}^2$ at even higher temperature of $T/T_c = 0.89$ [17]. The Co ions are substituted into the Fe-sites and induce additional scattering centers, which can be confirmed by the observation of the increased residual resistivity ($\sim 20 \mu\Omega \text{ cm}$ by extrapolating to $T = 0$). The impurity ions can work as pinning centers to restrict

the vortex motion. However, it seems like that the Co enhances the vortex motion and consequently decreases the J_c . We can conclude that the present J_c is in accordance with the J_c^{GL} , but not with the vortex motion profile. On the other hand, the J_c is quite sensitive to temperature, i.e., the slopes of dJ_c/dT are $5.13 \text{ MA/cm}^2 \text{ K}$ for the temperature below 22 K, which is comparable with the value obtained on the impurity-free crystal ($6.88 \text{ MA/cm}^2 \text{ K}$) [17].

We further studied the anisotropic factor of the J_c ($\gamma_J = J_c^{\text{ab}}/J_c^c$) as shown in Fig. 4. The γ_J demonstrates weak magnetic field dependence: (i) at the low field region below 0.2 T, the γ_J sharply increases with field from 1 to 1.5; (ii) at fields from 0.2 to 1.2 T, the γ_J gradually decreases down to 1.3 with increasing field; and (iii) the γ_J increases again with respect of field above 1.2 T. Note that the γ_J is ~ 1.7 for $\mu_0 H = 3 \text{ T}$, indicating slightly larger anisotropy than that of impurity-free crystal, for which the γ_J is ~ 1.26 for $\mu_0 H = 5 \text{ T}$. However, the present J_c anisotropy is substantially less than that of $\text{Fe}(\text{Se}, \text{Te})$ (~ 10 under 6 T) [4], $\text{Ba}(\text{Fe}, \text{Co})_2\text{As}_2$ (~ 2.6 under 4 T) [7], and $\text{LaFeAsO}_{1-x}\text{F}_x$ (~ 5 under 9 T) [8] thin films.

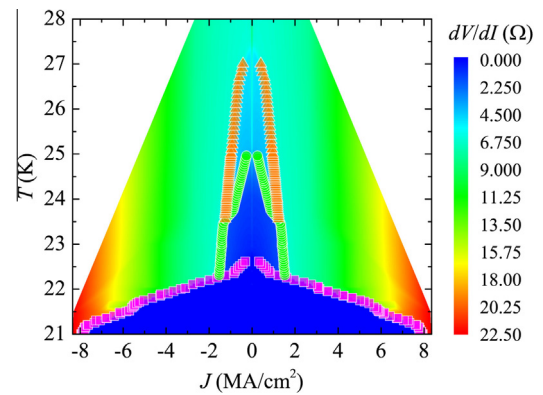


Fig. 3. Temperature and current densities dependent differential resistances for the microbridges. Here, we focus on the current sweep-up branches. The color contours represent the differential resistance dV/dI . The blue square points demonstrate the J_c for each voltage shunt, and the other points are consistent with the J_c of phase-slip centers. (For interpretation of the references to colour in this figure legend, the reader is referred to the web version of this article.)

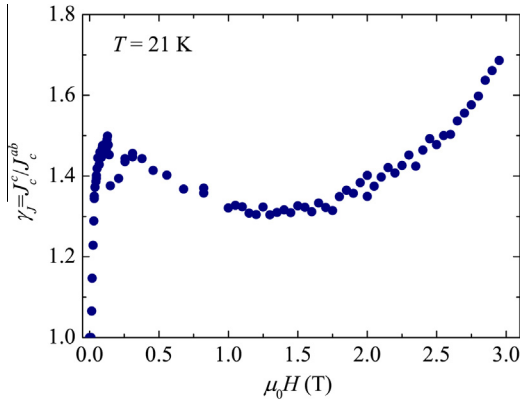


Fig. 4. J_c anisotropy of microbridges at various magnetic fields. Here all the data are obtained at 21 K and from the current sweep-up branches of IVCs.

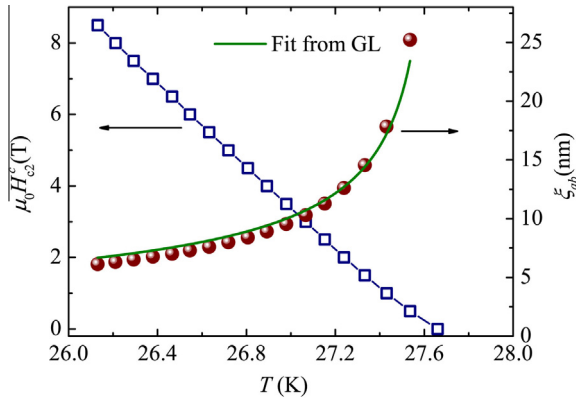


Fig. 5. Temperature dependence of the H_{c2}^c and the ξ_{ab} . Here, the H_{c2}^c is defined from the resistivity transition points at 90% of ρ_n (29 K) in Fig. 1, and the ξ_{ab} is calculated from the Ginzburg–Landau formula for an anisotropic three-dimensional superconductor $\xi_{ab}(T) = \sqrt{\Phi_0/2\pi H_{c2}^c(T)}$. We also fit the $\xi_{ab}(T)$ by the Ginzburg–Landau theory $\xi(T) = \xi_0(T)/\sqrt{(1-T/T_c)}$ as shown by green line in the figure. (For interpretation of the references to colour in this figure legend, the reader is referred to the web version of this article.)

Considering the quasi-one-dimensional limit, we calculated the temperature dependence of $\xi(T)$ from the upper critical fields as $\xi_c(T) = \sqrt{\Phi_0/2\pi H_{c2}^{ab}(T)}$ as shown in Fig. 5. The as-estimated $\xi(T)$ was also fitted by employing the GL theory of $\xi(T) = \xi_0(T)/\sqrt{(1-T/T_c)}$. Hence we can roughly evaluate $\xi_{ab} = 3.10$ nm at $T = 21$ K and $\xi_{ab} = 1.57$ nm at $T = 0$ K. However, the estimated ξ values are much smaller than sample sizes, for instance the thickness. Therefore, the present sample can hardly be treated as quasi-one-dimensional structure.

4. Conclusions

In conclusion, we studied transport properties of $\text{Ba}_{0.5}\text{K}_{0.5}\text{Fe}_{1.95}\text{Co}_{0.05}\text{As}_2$ microbridges with width of $2\ \mu\text{m}$ and thickness of

150 nm. The temperature dependence of resistivity demonstrates several steps and a broad superconducting transition with a width of 5 K. The current density vs. voltage characteristics of the microbridges showed a Josephson-like behavior with an obvious hysteresis. The critical current density at 21 K was found to be $J_c = 7.9\ \text{MA}/\text{cm}^2$, which is consistent with the Ginzburg–Landau depairing limit. The critical current density was found to be weakly field dependent with anisotropy factor of 1.3 (1 T) and 1.7 (3 T). Although the Co impurity ions increase the scattering rate within the superconducting Fe_2As_2 layers, they also decrease the critical current density compared with the pure crystal. The effect of Co impurity on the critical current density is related to a different mechanism of vortex pinning. We also found weak phase-slip behavior in Co-doped $\text{Ba}_{0.5}\text{K}_{0.5}\text{Fe}_2\text{As}_2$ microbridges, although the coherence length is far less than the sample size. However, such phenomenon can only be observed at temperatures near the T_c or in the return branch of the current density vs. voltage characteristic where the Joule heating effect is pronounced.

Acknowledgements

We thank Dr. V.N. Gladilin for valuable discussions. This research was supported by the from Methusalem Funding by the Flemish government, the World Premier International Research Center from MEXT, the Grants-in-Aid for Scientific Research (20360012, 22246083) from JSPS, the Funding Program for World-Leading Innovative R&D on Science and Technology (FIRST Program) from JSPS, Japanese–German International Cooperative Program of the JST and the DFG, the National Natural Science Foundation of China (No. 11234006).

References

- [1] Y. Kamihara, T. Watanabe, M. Hirano, H. Hosono, *J. Am. Chem. Soc.* **130** (2008) 3296.
- [2] J. Paglione, R.L. Greene, *Nat. Phys.* **6** (2010) 645.
- [3] I.I. Mazin, D.J. Singh, M.D. Johannes, M.H. Du, *Phys. Rev. Lett.* **101** (2008) 057003.
- [4] K. Iida et al., *Phys. Rev. B* **87** (2013) 104510.
- [5] D. Rall et al., *Phys. Rev. B* **83** (2011) 134514.
- [6] S. Lee et al., *Nat. Mater.* **9** (2010) 397.
- [7] T. Katase et al., *Nat. Commun.* **2** (2011) 409.
- [8] M. Kildszun et al., *Phys. Rev. Lett.* **106** (2011) 137001.
- [9] J.H. Durrell et al., *Rep. Prog. Phys.* **74** (2011) 124511.
- [10] H. Hilgenkamp, J. Mannhart, *Rev. Mod. Phys.* **74** (2002) 485.
- [11] C.P. Bean, *Rev. Mod. Phys.* **36** (1964) 31.
- [12] L. Fang et al., *Appl. Phys. Lett.* **101** (2012) 012601.
- [13] S. Nawaz, R. Arpaia, F. Lombardi, T. Bauch, *Phys. Rev. Lett.* **110** (2013) 167004.
- [14] M.Y. Kupriyanov, V.F. Lukichev, *Fiz. Nizk. Temp.* **6** (1980) 445; M.Y. Kupriyanov, V.F. Lukichev, *Sov. J. Low Temp. Phys.* **6** (1980) 210.
- [15] K.K. Likharev, *Rev. Mod. Phys.* **51** (1979) 101.
- [16] K. Xu, P. Cao, J.R. Heath, *Nano Lett.* **10** (2010) 4206.
- [17] J. Li et al., *Appl. Phys. Lett.* **103** (2013) 062603.
- [18] J. Li et al., *Phys. Rev. B* **85** (2012) 214509.
- [19] M. Tian et al., *Nano Lett.* **6** (2006) 2773.
- [20] A. Bezryadin, C.N. Lau, M. Tinkham, *Nature* **404** (2000) 971.
- [21] H. Kim, S. Jamali, A. Rogachev, *Phys. Rev. Lett.* **109** (2012) 027002.
- [22] J.A. Bonetti, D.S. Caplan, D.J. Van Harlingen, M.B. Weissman, *Phys. Rev. Lett.* **93** (2004) 087002.